High Resolution Eddy Current Testing of Superconducting Wires using GMR-Sensors

Marc Kreutzbruck
Federal Institute for Materials Research and Testing, 12205 Berlin, Germany

Kai Allweins, Chris Strackbein, Hendrik Bernau
Institute of Applied Physics, University of Giessen, 35390 Giessen, Germany
Tel: +49 30 81041840   Fax: +49 30 81041845
E-mail: marc.kreutzbruck@bam.de, Web: http://www.bam.de

Abstract:

In this work we present a reconstruction algorithm for a modern electromagnetic non-destructive testing approach using a small GMR sensor array to inspect superconducting wires. Four sensitive GMR sensors are positioned around the wire. Small defects of 100 µm in size could be detected in a depth of 200 µm with a signal-to-noise ratio of better than 400. Surface defects could be detected with a SNR of up to 10,000. This remarkably SNR and the small extent of GMR sensors results in a spatial resolution which offers new visualisation techniques for defect localisation, defect characterization and future tomography-like mapping techniques. We developed several inverse algorithms based on either a Finite Element Method or an analytical approach leading to defect localization with an accuracy of a few 10 µm.

Keywords: GMR-sensor, Eddy Current Testing, reconstruction, superconducting wires

1   INTRODUCTION

Conventional superconducting wires consist of a copper wire in which superconducting NbTi-filaments are embedded. If a filament is defect the current must flow around the defect part through the copper matrix of the wire giving rise to critical energy dissipation according to ohm's law. Therefore a testing method should provide information if the defect inside the wire injures the filaments and thus diminish the current transport properties. Especially when it comes to determine the size of a defect or its exact location, reliable imaging is vital for the decision if a defect might be unacceptable for the component's safe operation.

In case of wire testing one usually applies encircling testing coils with wire speeds of more than 1 m/s. Then the spatial resolution is limited due to the size of the detecting coil, because the voltage response signal will be an integral property in which each part of the coil section contributes. In doing so, one can not determine the size and position of the defect and no conclusion of the degree of damage can be obtained. As a way out we illuminate a new idea and an example of modern electromagnetic Non destructive Testing (NDT). The superconducting wires are tested using tiny GMR-sensors, which

locally resolve the field distribution around the wire. Thus, small and sensitive sensors with high spatial resolution and high signal-to-noise ratio pave the way for powerful inverse algorithms gaining deeper insight into the type of defect, its size and its location. GMR technique was already used in specific NDE-application [1-5].

2   EXPERIMENTAL SETUP

Figure 1 shows the arrangement of the four GMR-sensors. The excitation coil –not shown here- is connected to the low noise excitation unit, which generates eddy currents in the wire being tested. A lock-in-amplifier having a dynamic range of up to 110 dB/$\sqrt{}$Hz then compares the reference excitation signal with the measured field and its changes in amplitude and phase. The two output channels (in phase and quadrature) of each sensor are connected with a standard 18 bit data acquisition system.

The EC-measurement was performed with an encircling excitation coil and four GMR sensors to detect the radial component of the response field. The GMR sensors were positioned at 0°, 90°, 180 ° and 270 ° around the wire with a sensor-to-wire distance of about 150 µm. In order to preserve the total dynamic range of the lock-in amplifier for the detection of the response field variation, the excitation field was geometrically compensated. For this purpose the GMR sensors were attached exactly between the two halves of the encircling excitation coils, where the excitation field was quite low. The intrinsic field sensitivity of the GMR sensors was approximately 200 pT/$\sqrt{}$Hz for frequencies higher than 1 kHz and the spatial resolution of about 100 µm corresponds with the size of the active GMR-layer. Optimum excitation frequencies were determined by Finite-Element simulations to be 3 kHz for a wire thickness of about 5 mm and 300 kHz when testing wires with a thickness of about 500 µm.

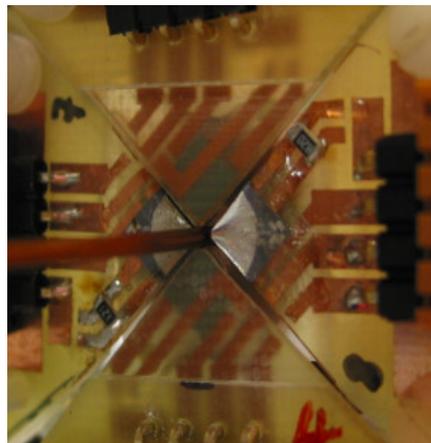Fig. 1. Four GMR sensors are attached around the wire with a sensor-to-wire distance of 150 µm.

3   MEASUREMENT

Figures 2 and 3 show an example of four response fields of the GMR-sensors array. The wires were positioned such that the material defect passes through exactly below sensor 1 (s1), which is also defined as the 0°-position. Sensor 1 therefore detects the strongest signal due to the smallest distance between the defect and the GMR-Sensor. The signal strength of sensor 1 can be 100 times higher than the response of sensor 3 at the opposite side of the wire. We found that the signal strength as function of the defect-to-sensor distance can be described by a $1/r^2$ law.

The maximum signal strength generated by surface defects with a lateral size of about 200 x 500 µm was determined to approximately 80 µT, which corresponds to an SNR of almost 10,000 (Fig. 2). The smallest natural defect in our samples consists of a defect filament in a depth of about 0.2 mm with a size of about 100 µm, which results in signal amplitude of 4.5 µT (Fig. 3). Regarding the peak-to-peak noise level of 10 nT_{pp} (Integration time of 100 µs) this corresponds to a SNR of almost 450 for small under surface defects. The intrinsic noise level of the GMR-sensors is about 200 pT/√Hz, paving the way for high testing velocities.
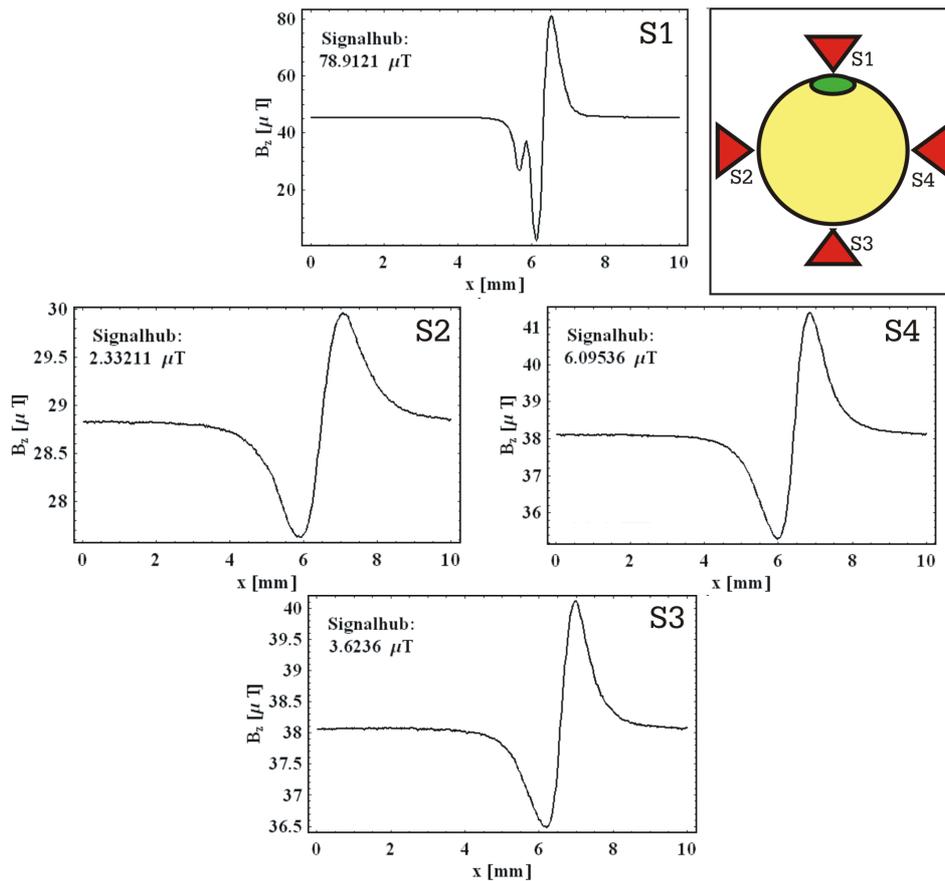
Fig. 2. Testing superconducting wires of 0.9 mm in diameter (wire A) . The sketch depicts the cross-section of the Cu-wire (NbTi-filaments are not shown) and the 4 GMR sensors. Magnetic field strength of the radial component as function of the axial wire position for each GMR sensor (s1 – s4). Defect size: 400 µm x 350 µm + small defect; both of them were surface defects.
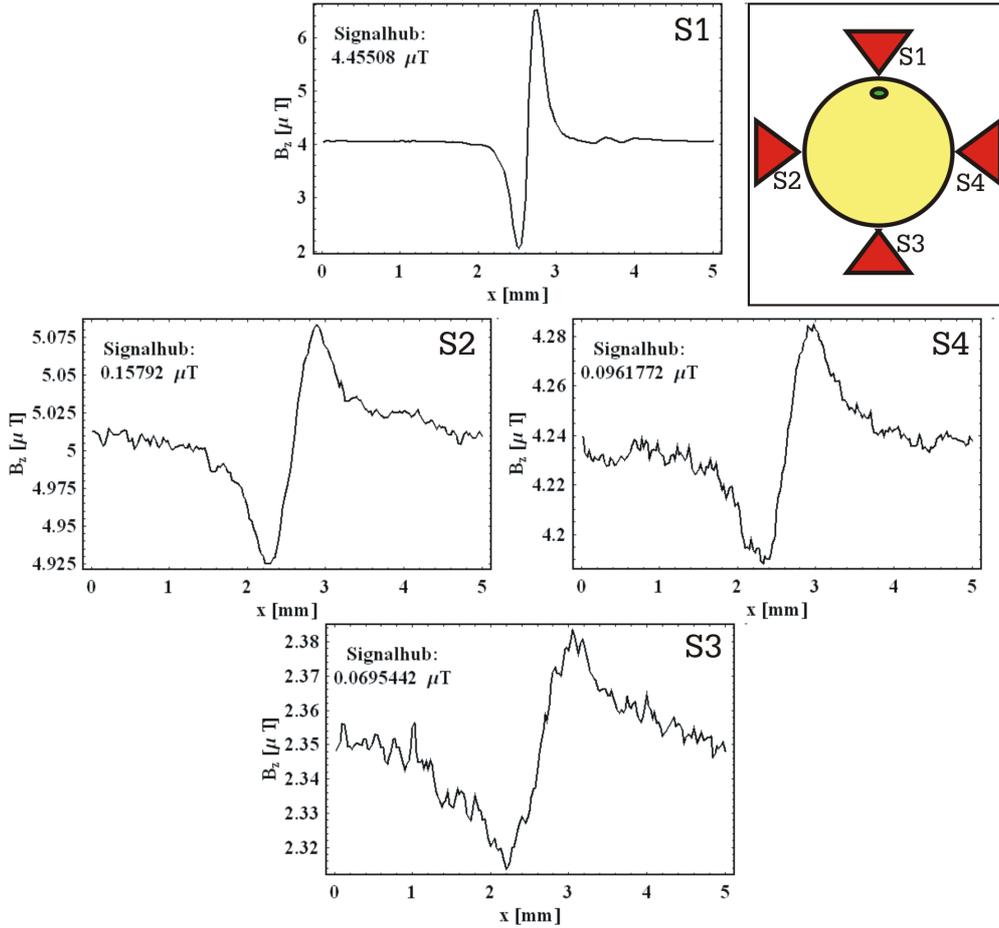
Fig. 3. Testing superconducting wires of 1.0 mm in diameter (wire B). The sketch depicts the cross-section of the Cu-wire (NbTi-filaments are not shown) and the 4 GMR sensors. Magnetic field strength of the radial component for each GMR sensor (s1 – s4) as function of the axial wire position. Defect size: 100 μm in a depth of about 200 μm.

4 INVERSE ALGORITHM

To determine whether a signal from a material defect is critical for either the function or the further production process, it is important to determine the position and the size of the defect. We studied both an analytical and a numerical inverse approach. The latter is based on a FEM-calculation and the assumption to deal with spherical defect shapes (Fig. 4, left). The analytical model assumes to have cylindrical defect shapes and uses conformal map techniques in conjunction with Bessel functions. A multipol expansion of the Biot-Savart-law and a first order approximation then determines the detected field strength at each sensor, from which we calculate the x/y-position of the defect. Both models provide an isoline map of the sensor amplitude ratios of different defect positions within the wire's cross section (Fig. 5, right). When determining the isolines of both pairs of diametrically placed sensors, the intersection of both isolines then reveals the position of the defect.
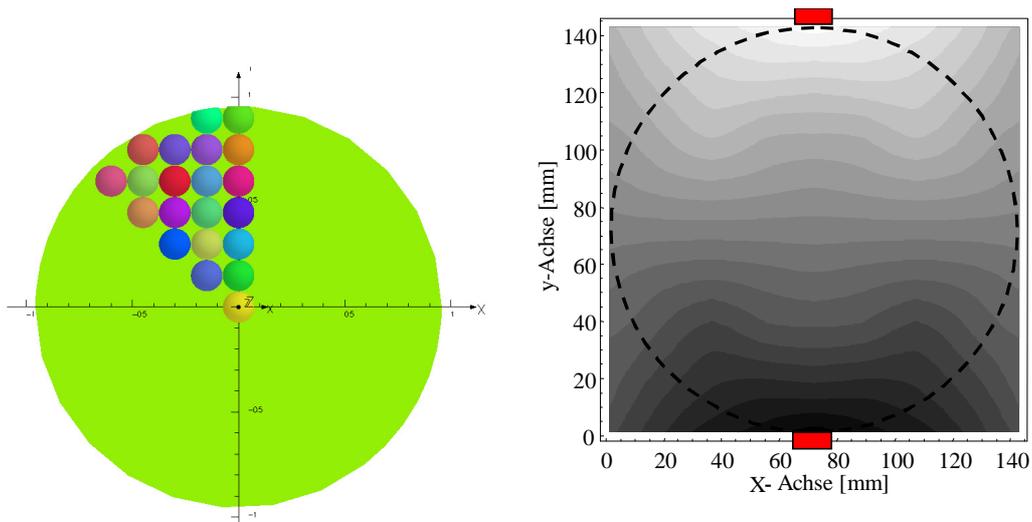
Fig. 4. Left: FEM-model to determine the signal strength for any defect position within the wire's cross-section. Right: Isoline map of amplitude ratio B_{s1}/B_{s3} of two diametrically placed sensors (on top and bottom of the wire with a diameter of 1.4 mm). The amplitude ratio S1/S3 is scaled from 1530 (white) to $6.54 \cdot 10^{-4}$ (black).

Figure 5 shows the reconstructed x/y position (r/φ) of the analytical inverse solution. In order to estimate the accuracy of the experimental findings and the influence of the defect position on the signal strength of each sensor, we rotate the wire after each measurement by 10° and start the measurement again. For each 10°-step up to a total rotation of 90° the position of the defect was again calculated. Thus we got 10 defect positions (red points in Fig. 5) which are expected to be located on a sector of a circle. From the position of the defect we can determine the defect's volume. Four wires were tested destructively, obtaining the exact position and the real defect shape and size.

1. The angle error φ is between 2% and 10%, depending on the defect's shape. Larger errors occur for complex defect shapes (see Fig. 5, right).

2. The *x/y*-position was found for four wires and all 10 angle steps with an average accuracy of ± 30 µm, depending on the deviations from a spherical or cylindrical defect shape.

3. The volume of the defect was determined with an error of about ± 50%, corresponding to an accuracy of the defect diameter of about 15% (See Fig. 6). Besides the cross-section of the defect we can estimate the length of the defect by the width of the defect signal, obtaining a 3D-information of the defect.
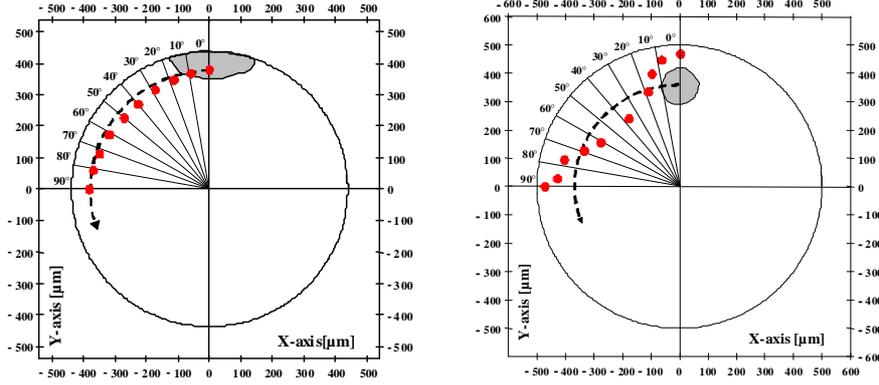
Fig. 5. Determination of the defect position (red circles) inside the wire for 10 different angles between the defect and the sensor 1. The wire was rotated in 10°-steps after each measurement. The grey area resembles the defect. Left: wire A, Right: wire B.
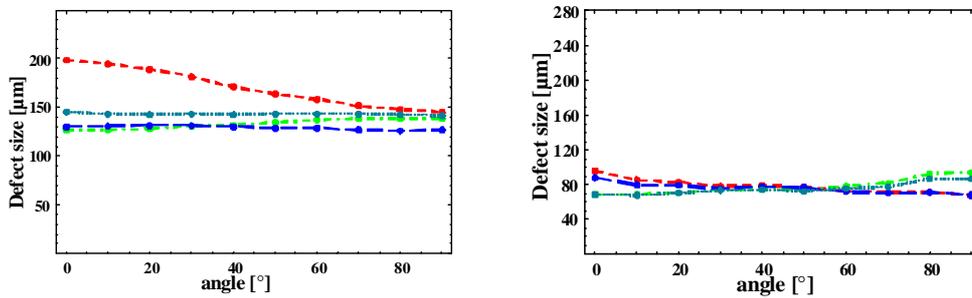

Fig. 6. Determination of the defect diameter as function of the angle position of the defect. Amplitude values of sensor S1 (dashed lines), S2 (points and lines), S3 (long lines), S4 (points). Left: wire A, Right: wire B.

5 CONCLUSIONS

The presented model and the small number of applied sensors, naturally do not allow for tomography-like images, but it proves that high signal-to-noise ratio in combination with good spatial resolution plays a major role for the interpretation of the detected field. Even when using only 4 sensors instead of an integral encircling detection coil, we obtain striking information about the defect. This helps to clarify if the defect injured the superconducting filaments inside the Cu-matrix. The results can be regarded as a first step towards the use of GMR sensor arrays containing a larger number of GMR-layers, which provide a more complete picture of the real magnetic field distribution of the sample's outside world. This paves the way for new visualisation techniques, precisely defect localisation, defect characterisation, and also future tomography-like mapping techniques.

REFERENCES

[1]   W. Ricken, J. Liu, W. J. Becker, EMSA 2000, Dresdner Beiträge zur Sensorik 13, 71-72 (2000)
[2]   C. H. Smith, R. W. Schneider, T. Dogaru, S. T. Smith, Rev. Prog. in QNDE, 22, 419-426, (2003)
[3]   B. Wincheski, M. Namkung, Rev. Prog. Quant. Nondestr. Eval. 509, 465 (2000)
[4]   Dogaru, T and Smith, S. T, *IEEE Trans. Magn,* 37, 3831 (2003)
[5]   K. Allweins, M. von Kreutzbruck, G. Lembke, J. Appl. Phys. 97, 10Q102 (2005)